Electronic Supplementary Material (ESI) for Dalton Transactions.

Design, synthesis and reactivity of dimolybdenum complex bearing quaterphenylene-bridged pyridine-based PNP-type pincer ligand

Aya Eizawa,[1] Kazuya Arashiba,[1] Hiromasa Tanaka,[2] Asuka Konomi,[3] Kazunari Yoshizawa,*[3] Yoshiaki Nishibayashi*[1]

[1] Department of Systems Innovation, School of Engineering, The University of Tokyo, Bunkyo-ku, Tokyo 113-8656, Japan

[2] Daido University, Takiharu-cho, Minami-ku, Nagoya, 457-8530, Japan

[3] Institute for Materials Chemistry and Engineering, Kyushu University, Nishi-ku, Fukuoka 819-0395, Japan.

Table of Contents

1. General information.

^{1}H NMR (400 MHz), ^{13}C{^{1}H} NMR (101 MHz), and ^{31}P{^{1}H} NMR (162 MHz) spectra were recorded on a JEOL JNM-ECS 400 spectrometer in suitable solvents, and spectra were referenced to residual solvent (^{1}H, ^{13}C) or external standard (^{31}P{^{1}H}: H_3PO_4). Magnetic susceptibility was measured in CD_2Cl_2 using the Evans method.[S1] Flash column chromatography was carried out on a Yamazen YFLC-AI-580 system. Absorption spectra were recorded on a Shimadzu UV-1850. Evolved dihydrogen was quantified by a gas chromatography using a Shimadzu GC-8A with a TCD detector and a SHINCARBON ST (6 m × 3 mm). Elemental analyses were performed at Microanalytical Center of The University of Tokyo. Melting points were measured by using a Stanford Research Systems OptiMelt MPA100.

All manipulations were carried out under an atmosphere of nitrogen or argon by using standard Schlenk techniques or glovebox techniques unless otherwise stated. Solvents were dried by general methods and degassed before use. 4-(4,4,5,5-tetramethyl-1,3,2-dioxaborolan-2-yl)-2,6-bis(di-*tert*-butylphosphinothioylmethyl)pyridine (PNP(S)-Bpin),[S2] [$MoX_3(thf)_3$] (X = Cl[S3], I[S4]), [$MoCl_3$(PNP)] (**6**, PNP = $C_5NH_3(CH_2P^tBu_2)_2$),[S5] [$MoCl_3$(Ph-PNP)] (**7**, Ph-PNP = 4-Ph-$C_5NH_2(CH_2P^tBu_2)_2$),[S2] and $SmI_2(thf)_2$[S6] were prepared according to the literature methods. All the other reagents were commercially available.

2. Experimental procedures.

Synthesis of 2

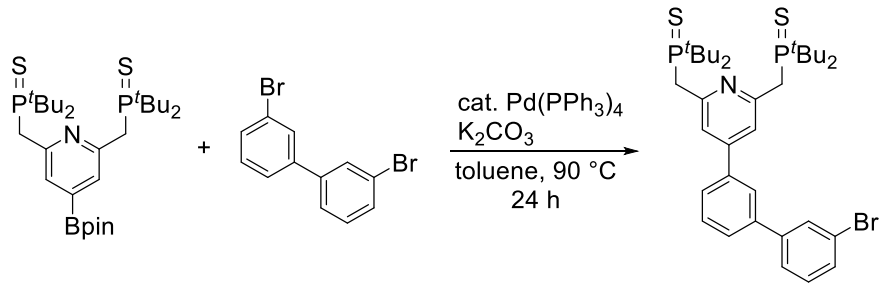

PNP(S)-Bpin **2**

To a mixture of PNP(S)-Bpin (4.23 g, 7.2 mmol), 2,2′-dibromobiphenyl (3.15 g, 10 mmol), $Pd(PPh_3)_4$ (1.17 g, 1.0 mmol), and K_2CO_3 (4.98 g, 36 mmol) was added toluene (140 mL), and the suspension was stirred at 90 ˚C for 24 h. The reaction mixture was cooled to room temperature, and water was added to the reaction mixture. The organic layer was extracted with toluene (20 mL x 3), and the combined solution was dried with anhydrous $MgSO_4$. The solution was filtered, and volatiles were removed. Purification with column chromatography (hexane/AcOEt = 3/1) and recrystallization from hot EtOH afforded **2** as colorless crystals (2.90 g, 4.2 mmol, 58% yield, mp 181.5-182.5 ˚C). ^{1}H NMR (C_6D_6): δ 8.43 (s, 2H, Ar*H*), 8.31 (s, 1H, Ar*H*), 8.01 (dt, *J* = 7.2 Hz, 1.6

Hz, 1H, Ar*H*), 7.75 (t, *J* = 2.0 Hz, 1H, Ar*H*), 7.40 (d, *J* = 8.4 Hz, 1H, Ar*H*), 7.19–7.10 (m, 3H, Ar*H*), 6.76 (dt, *J* = 7.6 Hz, 1.6 Hz, 1H, Ar*H*), 3.45 (d, $^{2}J_{PH}$ = 11.6 Hz, 4H, CH_2P), 1.19 (d, $^{3}J_{PH}$ = 14.4 Hz, 36H, P^t*Bu*$_2$). ^{13}C{^{1}H} NMR (acetone-d_6): δ 155.2 (d, *J* = 5.8 Hz), 146.6, 143.7, 141.0, 140.2, 131.7, 131.4, 130.7, 130.6, 128.4, 127.4, 126.7, 126.5, 123.5, 122.8, 38.9 (d, *J* = 41.7 Hz), 34.3 (d, *J* = 35.7 Hz), 28.0. ^{31}P{^{1}H} NMR (C_6D_6): δ 77.7 (s, *P*^{t}Bu$_2$). Anal. Calcd for $C_{35}H_{50}BrNP_2S_2$: C, 60.86; H, 7.30; N, 2.03. Found: C, 61.21; H, 7.42; N, 1.82.

Synthesis of 3

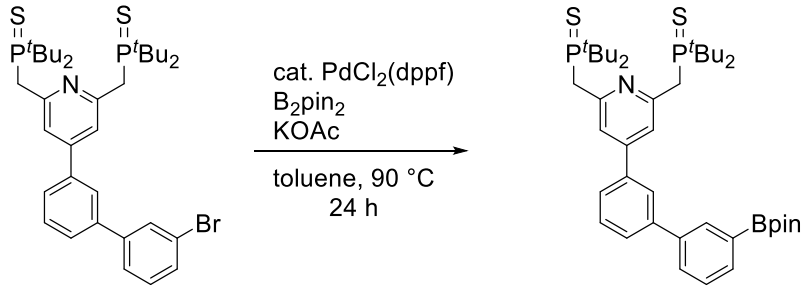

2 **3**

To a mixture of **2** (1046 mg, 1.5 mmol), bis(pinacolato)diboron (387 mg, 1.5 mmol), $PdCl_2$(dppf) (112 mg, 0.15 mmol), and KOAc (747 mg, 7.6 mmol) was added toluene (45 mL), and the suspension was stirred at 90 ˚C for 24 h. The reaction mixture was cooled to room temperature and filtered through Florisil. Volatiles were removed under vacuum to afford orange oil. Hexane (30 mL) was added to the oil, and the mixture was stirred at 50 ˚C to form beige precipitates. After cooling to room temperature, the resultant suspension was filtered, washed with hexane (5 mL x 2), and dried in vacuo to give **3** as a beige solid (850 mg, 1.2 mmol, 76% yield, mp 209.5-210.5 ˚C). ^{1}H NMR (C_6D_6): δ 8.55 (s, 1H, Ar*H*), 8.45 (s, 1H, Ar*H*), 8.40 (s, 2H, Ar*H*), 8.07 (d, *J* = 7.2 Hz, 1H, Ar*H*), 7.98 (d, *J* = 8.4 Hz, 1H, Ar*H*), 7.77 (d, *J* = 7.6 Hz, 1H, Ar*H*), 7.43 (d, *J* = 8.4 Hz, 1H, Ar*H*), 7.23 (t, *J* = 7.6 Hz, 1H, Ar*H*), 7.15 (t, *J* = 7.6 Hz, 1H, Ar*H*), 3.43 (d, $^{2}J_{P-H}$ = 11.2 Hz, 4H, CH_2P), 1.20 (d, $^{3}J_{PH}$ = 14.4 Hz, 36H, P^t*Bu*$_2$), 1.18 (s, 12H, B*pin*). ^{13}C{^{1}H} NMR (acetone-d_6): δ 155.2 (d, *J* = 5.7 Hz), 146.8, 142.6, 140.7, 140.1, 134.6, 134.1, 130.63, 130.57, 129.3, 128.3, 126.8, 126.5, 122.8, 84.6, 38.9 (d, *J* = 41.4 Hz), 34.3 (d, *J* = 35.7 Hz), 28.0, 25.2, the carbon directly connected to the boron was not detected. ^{31}P{^{1}H} NMR (C_6D_6): δ 77.6 (s, *P*^{t}Bu$_2$). Anal. Calcd for $C_{41}H_{62}BNO_2P_2S_2$: C, 66.74; H, 8.47; N, 1.90. Found: C, 66.49; H, 8.44; N, 2.02.

Synthesis of 4

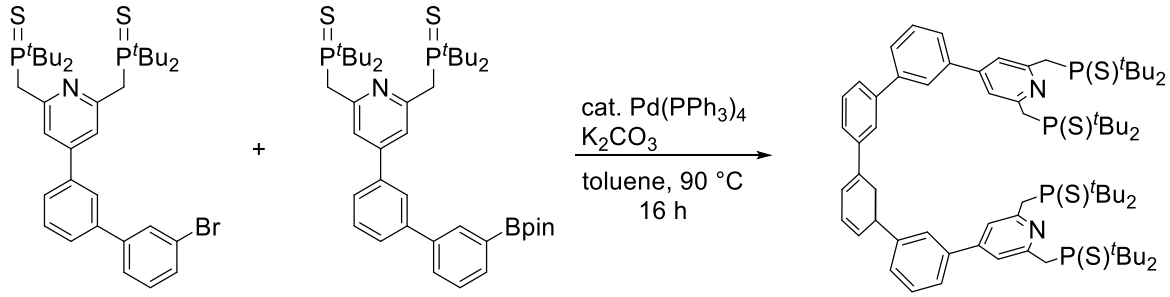

2 **3** **4**

To a mixture of **2** (690 mg, 1.0 mmol), **3** (738 mg, 1.0 mmol), $Pd(PPh_3)_4$ (116 mg, 0.10 mmol), and K_2CO_3 (694 mg, 5.0 mmol) was added toluene (40 mL), and the suspension was stirred at 90 °C for 16 h. The reaction mixture was cooled to room temperature, and water was added to the reaction mixture. The organic layer was extracted with toluene (5 mL x 3), and the combined solution was dried with anhydrous $MgSO_4$. The extract was filtered, and volatiles were removed. Purification with column chromatography (hexane/AcOEt = 3/1 to 1/1) gave a colorless oil. EtOH (200 mL) was added to the oil, and the mixture was stirred at 75 ˚C to form white precipitates. After cooling to room temperature, the resultant suspension was filtered, washed with hexane (5 mL x 3), and dried in vacuo to afford **4** as a white solid (478 mg, 0.39 mmol, 39% yield, mp 277.0-278.0 ˚C). ^{1}H NMR (C_6D_6): δ 8.59 (s, 2H, ArH), 8.50 (s, 4H, ArH), 8.09 (d, J = 7.2 Hz, 2H, ArH), 8.08 (s, 2H, ArH), 7.67 (d, J = 7.6 Hz, 2H, ArH), 7.61 (d, J = 7.6 Hz, 2H, ArH), 7.55 (d, J = 7.6 Hz, 2H, ArH), 7.34 (t, J = 7.6 Hz, 2H, ArH), 7.27 (d, J = 7.6 Hz, 2H, ArH), 3.46 (d, $^2J_{PH}$ = 11.2 Hz, 8H, CH_2P), 1.20 (d, $^3J_{PH}$ = 14.4 Hz, 72H, P^t*Bu*$_2$). ^{13}C{^{1}H} NMR (CD_2Cl_2): δ 154.4 (d, J = 6.7 Hz), 146.9, 142.04, 141.96, 141.6, 139.3, 129.9, 129.8, 128.1, 126.9, 126.6 (overlapping), 126.5, 126.4, 122.4, 38.6 (d, J = 40.5 Hz), 34.3 (d, J = 34.7 Hz), 27.9. ^{31}P{^{1}H} NMR (C_6D_6): δ 77.7 (s, *P*^{t}Bu$_2$). Anal. Calcd for $C_{70}H_{100}N_2P_4S_4$: C, 68.82; H, 8.25; N, 2.29. Found: C, 68.59; H, 8.38; N, 2.29.

Synthesis of 5

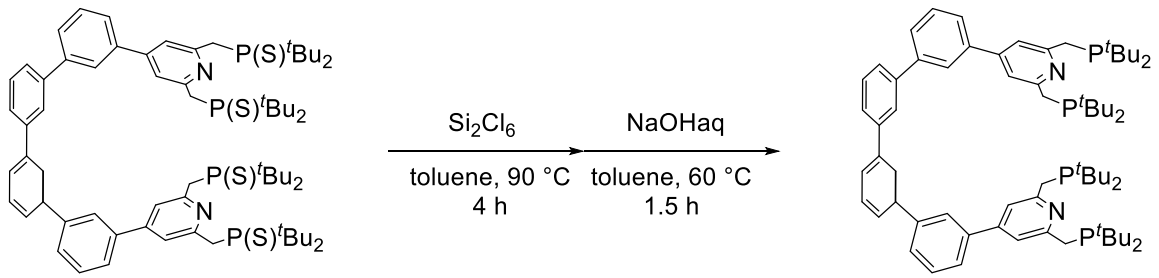

4 **5**

To a solution of **4** (214 mg, 0.17 mmol) in toluene (3 mL) was added Si_2Cl_6 (0.90 mL, 5.2 mmol), and the mixture was stirred at 90 °C for 4 h. The resultant solution containing red oil was

cooled to 0 °C. Aqueous NaOH solution (10 M, 10.5 mL, 105 mmol) was added dropwise, and the mixture was stirred at 60 °C for 1.5 h. The organic layer was extracted with toluene (2 mL x 3) and dried with anhydrous Na_2SO_4. The solution was filtered, and volatiles were removed under vacuum to give colorless oil. The oil was dissolved in benzene (3 mL), and then the solution was lyophilized to afford **5** as a white solid (108 mg, 0.10 mmol, 57% yield). This compound was used as a ligand without further purification. ^{1}H NMR (C_6D_6): δ 8.07 (s, 2H, Ar*H*), 7.87 (s, 2H, Ar*H*), 7.80 (s, 4H, Ar*H*), 7.62 (d, J = 7.6 Hz, 2H, Ar*H*), 7.49–7.42 (m, 6H, Ar*H*), 7.23 (t, J = 7.6 Hz, 4H, Ar*H*), 3.23 (d, J = 2.0 Hz, 8H, CH_2P), 1.16 (d, $^3J_{PH}$ = 10.4 Hz, 72H, P^t*Bu*$_2$). ^{31}P{^{1}H} NMR (C_6D_6): δ 35.7 (s, *P*^{t}Bu$_2$).

Synthesis of 1.

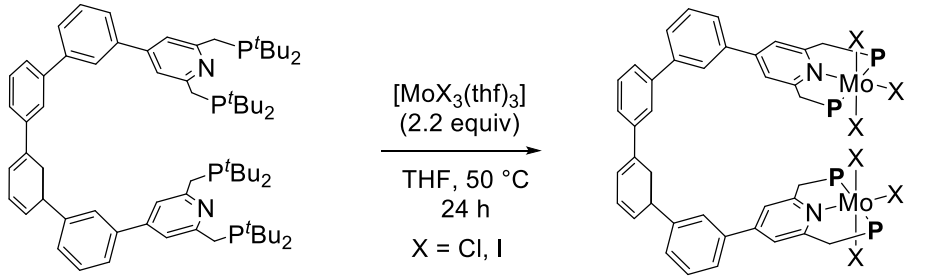

5 **1a**: X = Cl, **1b**: X = I; **P** = P^{t}Bu$_2$

A typical procedure for the synthesis of **1a** is described below. A mixture of **5** (35 mg, 0.032 mmol) and [$MoCl_3$(thf)$_3$] (30 mg, 0.071 mmol) in THF (3 mL) was stirred at 50 °C for 24 h. The solution was removed under vacuum, and the residue was washed with hexane (2 mL x 3). The resultant solid was extracted with THF (3 mL), and slow addition of benzene (3 mL) and hexane (15 mL) to the extract afforded **1a** as a red crystalline solid (29 mg, 0.019 mmol, 60% yield). Magnetic susceptibility (Evans method): μ_{eff} = 3.44μ_B in CD_2Cl_2 at 293 K. Analytical sample was obtained by recrystallization from THF-benzene-Et_2O. Anal. calcd for $C_{70}H_{100}Cl_6Mo_2N_2P_4$: C, 56.12; H, 6.73; N, 1.87. Found: C, 56.24; H, 6.70; N, 1.94.

8b: Recrystallization from THF-hexane gave **1b**·2C_6H_{14} as orange-brown crystals suitable for X-ray analysis. The crystals were filtered and dried in vacuo to afford **1b**·C_6H_{14} as a brown solid (60% yield). Magnetic susceptibility (Evans method): μ_{eff} = 3.43μ_B in CD_2Cl_2 at 293 K. Anal. calcd for $C_{76}H_{114}I_6Mo_2N_2P_4$: C, 42.80; H, 5.39; N, 1.31. Found: C, 43.32; H, 5.46; N, 1.32.

Catalytic reduction of dinitrogen to ammonia under N_2 atmosphere

A typical experimental procedure for the catalytic reduction of dinitrogen into ammonia using **1a** is described below. In a nitrogen-filled glove box, to a mixture of **1a** (1.5 mg, 0.0010 mmol (0.0020 mmol/Mo)) and SmI_2(thf)$_2$ (197.5 mg, 0.36 mmol) placed in a 50 ml Schlenk flask was added THF

(5.5 ml). The Schlenk flask was brought outside the glovebox, and THF (500 μl) containing H_2O (0.36 mmol) was added to the solution under N_2 (1 atm). The mixture was stirred at 25 ˚C for 18 h. After the reaction, the amount of dihydrogen obtained was determined by GC analysis (0.0088 mmol, 4 equiv/Mo). Aqueous solution of potassium hydroxide (30 wt%; 5 mL) was added to the reaction mixture, and the mixture was distilled into the dilute H_2SO_4 solution (0.5 M, 10 mL). The amount of NH_3 present in the H_2SO_4 solutions was determined by the indophenol method.[S7] The amount of ammonia was 0.112 mmol (56 equiv/Mo). The results of catalytic reaction are shown in Table S1.

Table S1. Catalytic reaction for ammonia production.

N_2 (1 atm) + 6 $SmI_2(thf)_2$ (0.36 mmol) + 6 H_2O (0.36 mmol) —Catalyst, THF, 25 °C, 18 h→ 2 NH_3 (+ H_2)

Catalyst	Cat load. (μmol/Mo)	NH_3 (mmol)	NH_3 (equiv/Mo)	NH_3 yield[a] (%)	H_2 (mmol)	H_2 (equiv/Mo)	H_2 yield[a] (%)
1a	2.0	0.108	54	90	0.016	8	9
1a	2.0	0.103	52	86	0.018	9	10
1a	2.0	0.112	56	93	0.0088	4	5
		average	54 ± 2	90 ± 4	average	7 ± 2	8 ± 3
1b	2.0	0.050	25	42	0.092	46	51
1a	0.20	0.100	500	83	0.018	90	10
1a	0.10	0.088	880	73	0.051	510	28
1a	0.10	0.078	780	65	0.049	490	27
		average	830 ± 70	69 ± 6	average	500 ± 10	28 ± 1
1a	0.050	0.0835	1670	70	0.043	860	24
1a	0.050	0.0840	1680	70	0.041	820	23
1a	0.050	0.0810	1620	68	0.045	900	25
		average	1660 ± 30	69 ± 1	average	860 ± 40	24 ± 1
6	0.050	0.033	660	28	0.039	780	22
6	0.050	0.037	740	31	0.031	620	17
6	0.050	0.035	700	30	0.029	580	16
		average	700 ± 40	29 ± 2	average	660 ± 110	18 ± 3
7	0.050	0.0895	1790	75	0.036	720	20
7	0.050	0.0944	1890	79	0.029	580	16
		average	1840 ± 70	77 ± 3	average	650 ± 100	18 ± 3

[a]Yield based on $SmI_2(thf)_2$.

3. X-ray crystallographic studies.

Crystallographic data of **1a**·$2C_6H_6$ and **1b**·$2C_6H_{14}$ is summarized in Table S2. The ORTEP drawing and selected bond lengths and angles are shown in Figures S1-2 and Tables S3-S4, respectively. Diffraction data were collected for the 2θ range of 4˚ to 63˚ at –180 °C on a Rigaku XtaLAB Synergy HPC diffractometer with graphite-monochromated Mo Kα radiation (λ = 0.71075 Å), with VariMax optics. Intensity data were corrected for Lorenz-polarization effects and for empirical absorption (ABSCOR). The structure solution and refinements were carried out by using the *CrystalStructure* crystallographic software package.[S8] The positions of the non-hydrogen atoms were determined by direct methods (SIR 2011[S9] for **1a**, SHELXS[S10] for **1b**) and subsequent Fourier syntheses (SHELXL 2016/9[S11]) and were refined on F_o^2 using all unique reflections by full-matrix least-squares with anisotropic thermal parameters. All the hydrogen atoms were placed at the calculated positions with fixed isotropic parameters.

The unit cell of **1a** or **1b** contains solvent accessible voids of 2046 Å^3 or 1617 Å^3, respectively. The electron density associated with some solvent molecules was removed by the SQUEEZE routine of PLATON[S12] for crystal data of **1a** and **1b**.

Table S2. X-ray crystallographic data for **1a** and **1b.**

	1a·2C_6H_6	**1b**·2C_6H_{14}
CCDC number	2279663	2279664
chemical formula	$C_{82}H_{112}Cl_6Mo_2N_2P_4$	$C_{82}H_{128}I_6Mo_2N_2P_4$
formula weight	1654.29	2219.13
dimensions of crystals	0.098 × 0.074 × 0.040	0.209 × 0.087 × 0.057
crystal color, habit	orange, plate	orange, needle
crystal system	monoclinic	monoclinic
space group	*I*2/a	*I*2/a
a, Å	17.0001(3)	17.9320(4)
b, Å	19.0388(3)	19.0778(4)
c, Å	30.0601(5)	30.6795(8)
α, deg	90	90
β, deg	103.092(2)	105.233(2)
γ, deg	90	90
V, Å^3	9476.4(4)	10126.8(4)
Z	4	4
ρ_{calcd}, g cm^{-3}	1.159	1.455
F(000)	3456.00	4384.00
μ, cm^{-1}	5.378	21.760
trans. factors range	0.778-0.979	0.103-0.883
no. reflections measured	40947	49727
no. unique reflections	11772 (R_{int}= 0.0414)	13312 (R_{int}= 0.0870)
no. parameters refined	433	433
*R*1 ($I > 2\ \sigma(I)$)[a]	0.0405	0.0683
*wR*2 (all data)[b]	0.1139	0.1911
GOF (all data)[c]	1.037	1.003
max diff peak / hole, e Å^{-3}	0.80/-0.42	2.37/-1.04

[a] $R1 = \Sigma||F_o|-|F_c||/\Sigma|F_o|$. [b] $wR2 = [\Sigma w(F_o^2-F_c^2)^2/\Sigma w(F_o^2)^2]^{1/2}$, $w = 1/[\sigma^2(F_o^2) + (qP)^2 + rP]$, $P = (\mathrm{Max}(F_o^2, 0) + 2\ F_c^2)/3$ [q = 0.0713 (**1a**), 0.1009 (**1b**); r = 3.5220 (**1a**), 0 (**1b**)]. [c] GOF = $[\Sigma w(F_o^2-F_c^2)^2/(N_o-N_{params})]^{1/2}$.

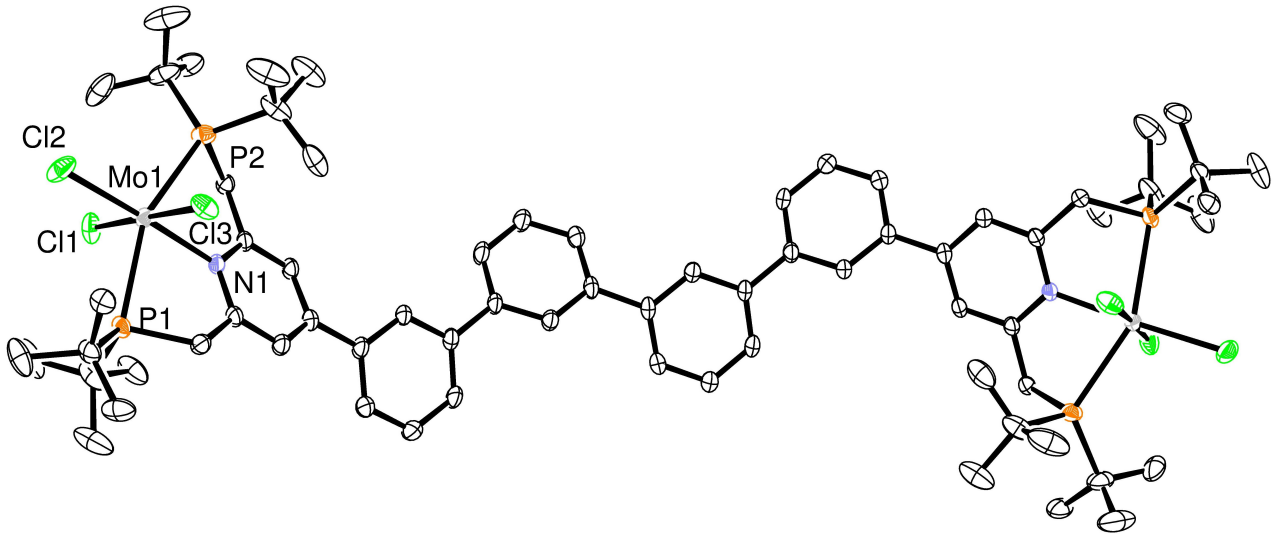

Figure S1. ORTEP drawing of **1a**. Thermal ellipsoids are shown at the 50% probability level. All hydrogen atoms are omitted for clarity.

Table S3. Selected bond lengths and angles of **1a**.

Bond lengths (Å)		Bond angles (deg)	
Mo1–Cl1	2.4269(7)	Cl1–Mo1–Cl3	176.86(3)
Mo1–Cl2	2.4044(7)	Cl2–Mo1–N1	177.33(6)
Mo1–Cl3	2.4253(7)	P1–Mo1–P2	154.22(2)
Mo1–P1	2.6033(8)		
Mo1–P2	2.6225(9)		
Mo1–N1	2.1872(16)		

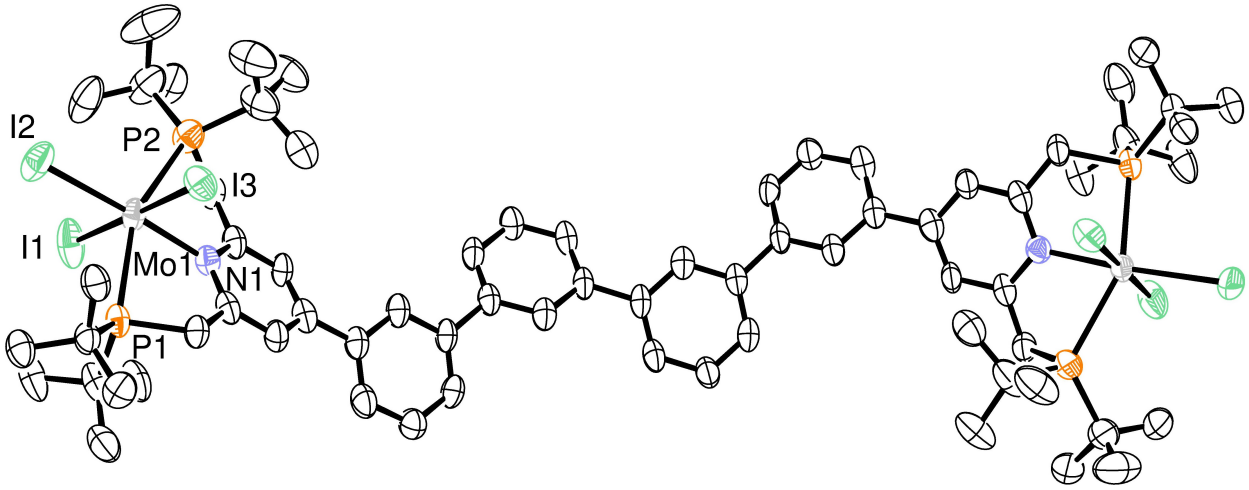

Figure S2. ORTEP drawing of **1b**. Thermal ellipsoids are shown at the 50% probability level. All hydrogen atoms are omitted for clarity.

Table S4. Selected bond lengths and angles of **1b**.

Bond lengths (Å)		Bond angles (deg)	
Mo1–I1	2.7740(8)	I1–Mo1–I3	179.26(3)
Mo1–I2	2.7498(7)	I2–Mo1–N1	176.12(13)
Mo1–I3	2.7834(7)	P1–Mo1–P2	153.77(5)
Mo1–P1	2.6329(18)		
Mo1–P2	2.683(2)		
Mo1–N1	2.180(4)		

4. NMR spectra.

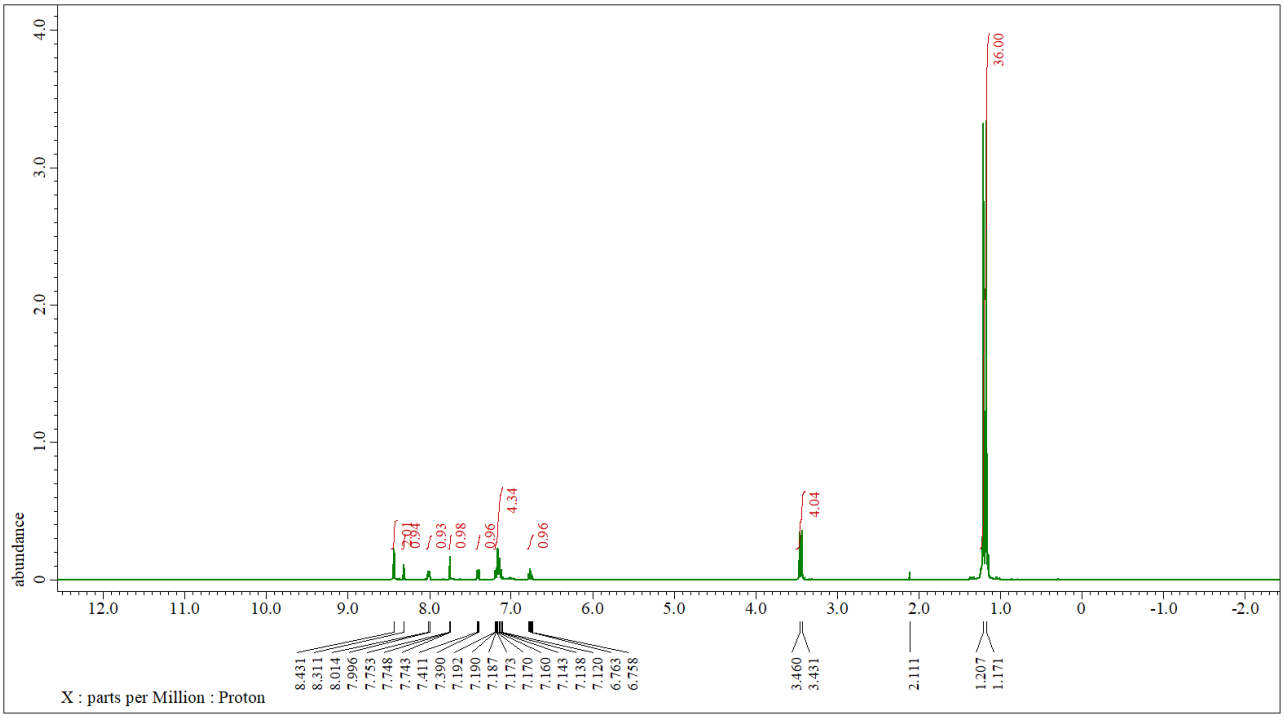

Figure S3. ^{1}H NMR spectrum of **2**.

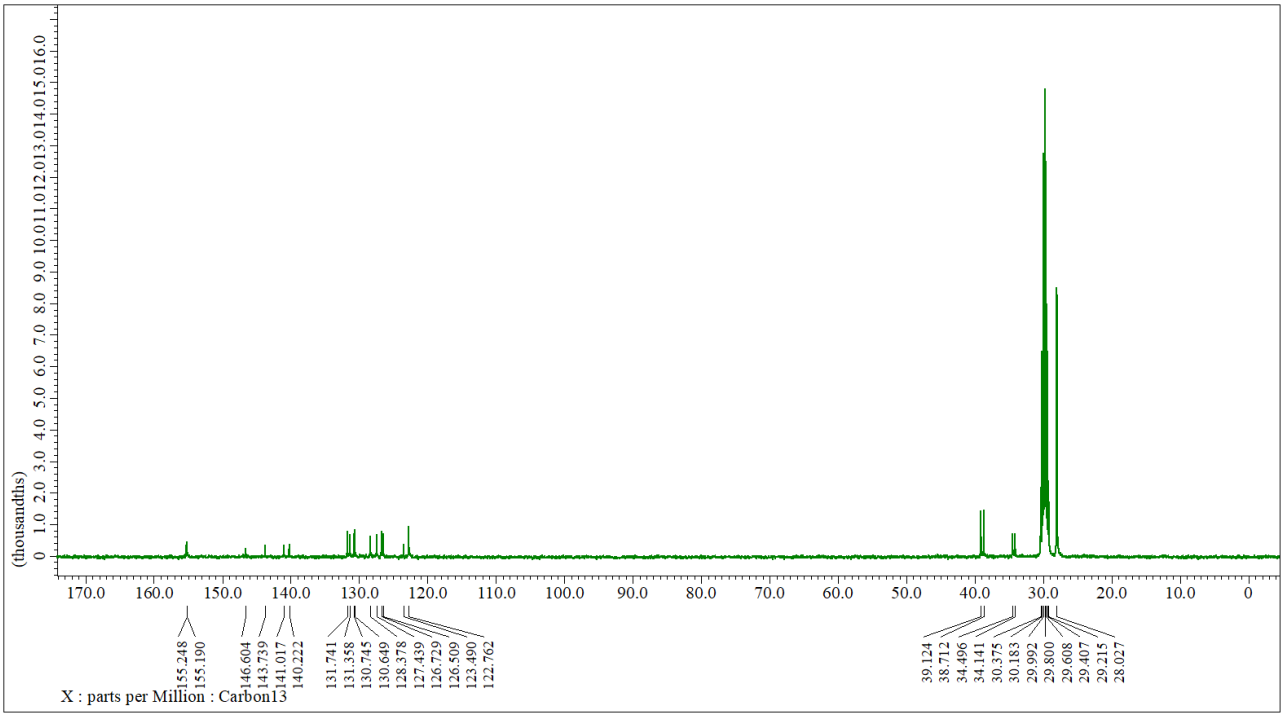

Figure S4. ^{13}C{^{1}H} NMR spectrum of **2**.

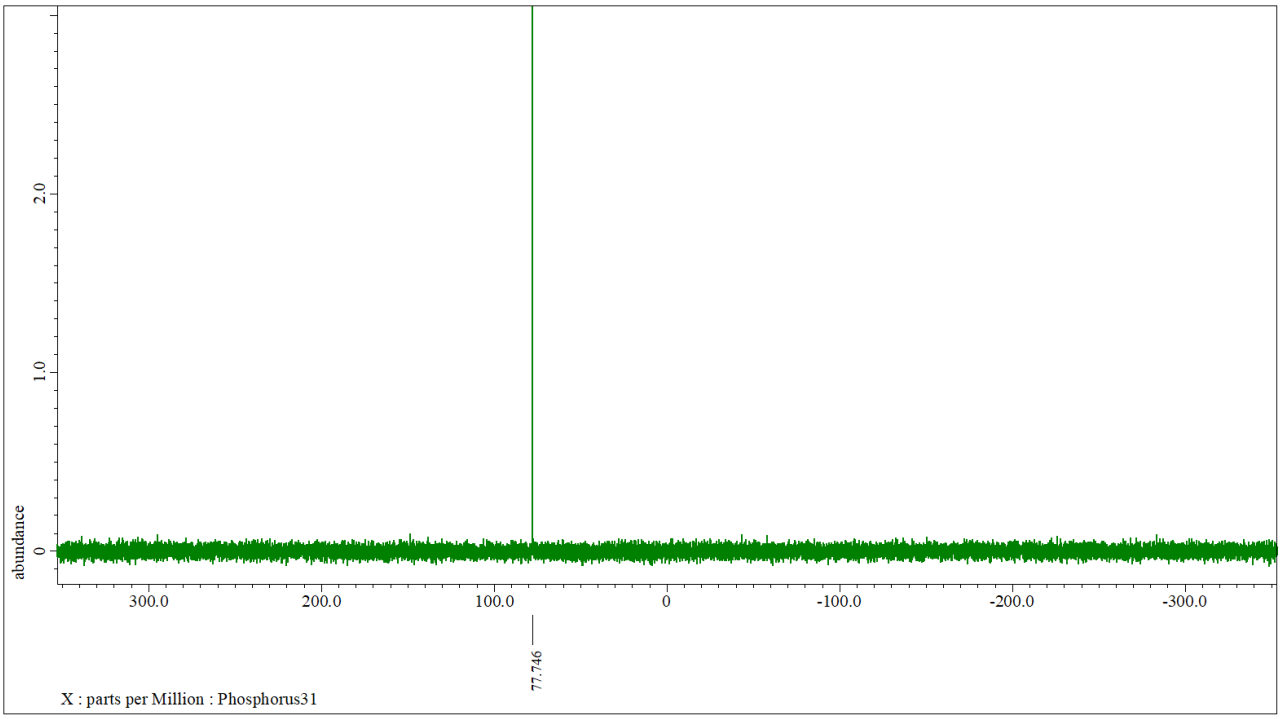

Figure S5. $^{31}P\{^{1}H\}$ NMR spectrum of **2**.

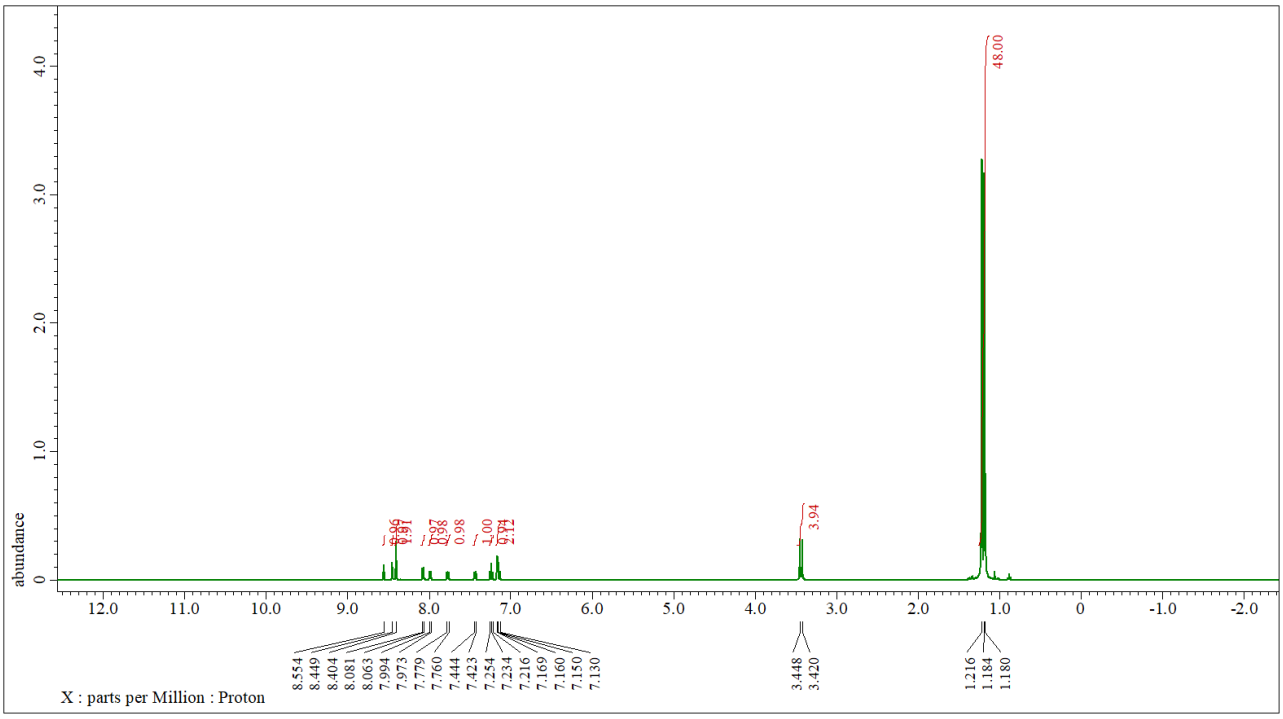

Figure S6. ^{1}H NMR spectrum of **3**.

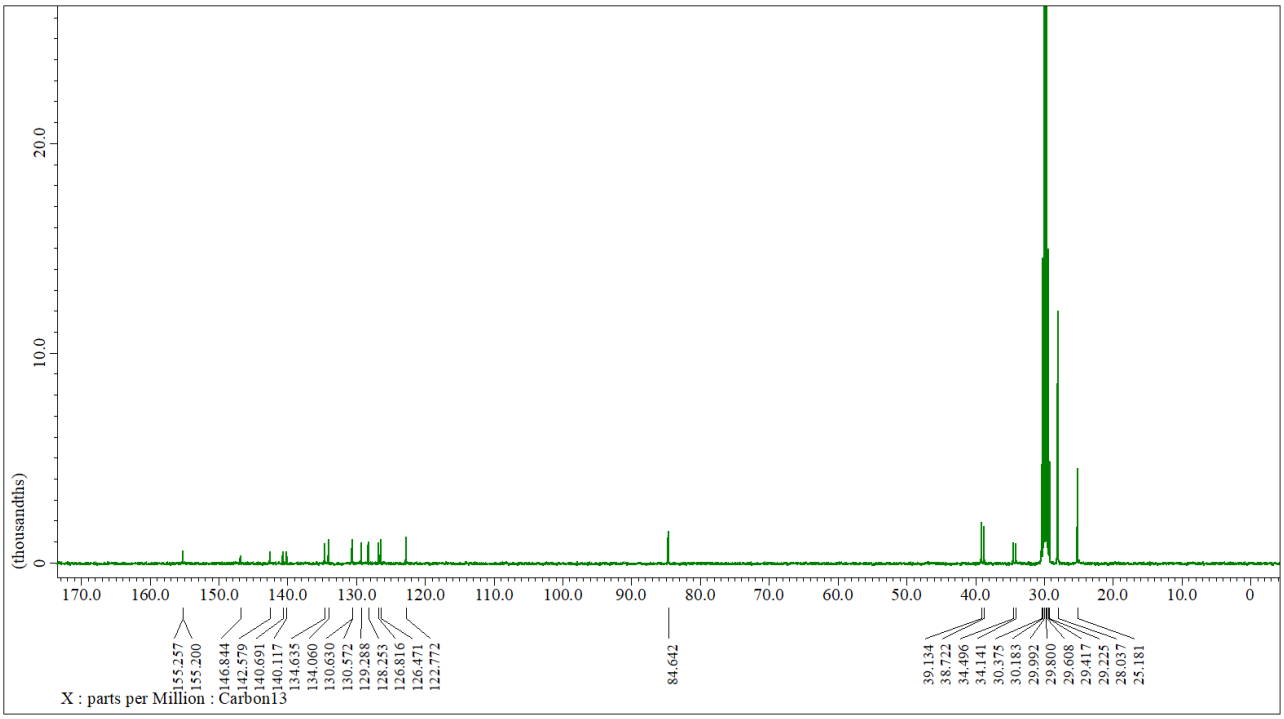

Figure S7. ^{13}C{^{1}H} NMR spectrum of **3**.

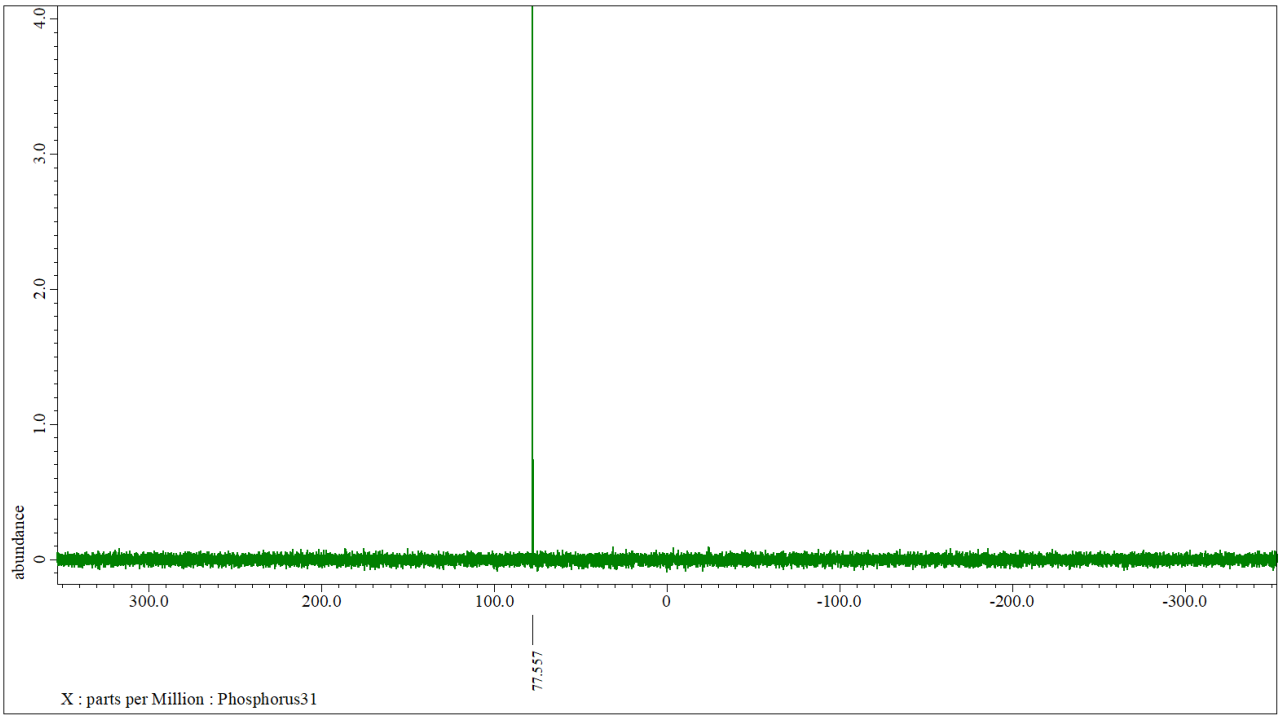

Figure S8. $^{31}P\{^{1}H\}$ NMR spectrum of **3**.

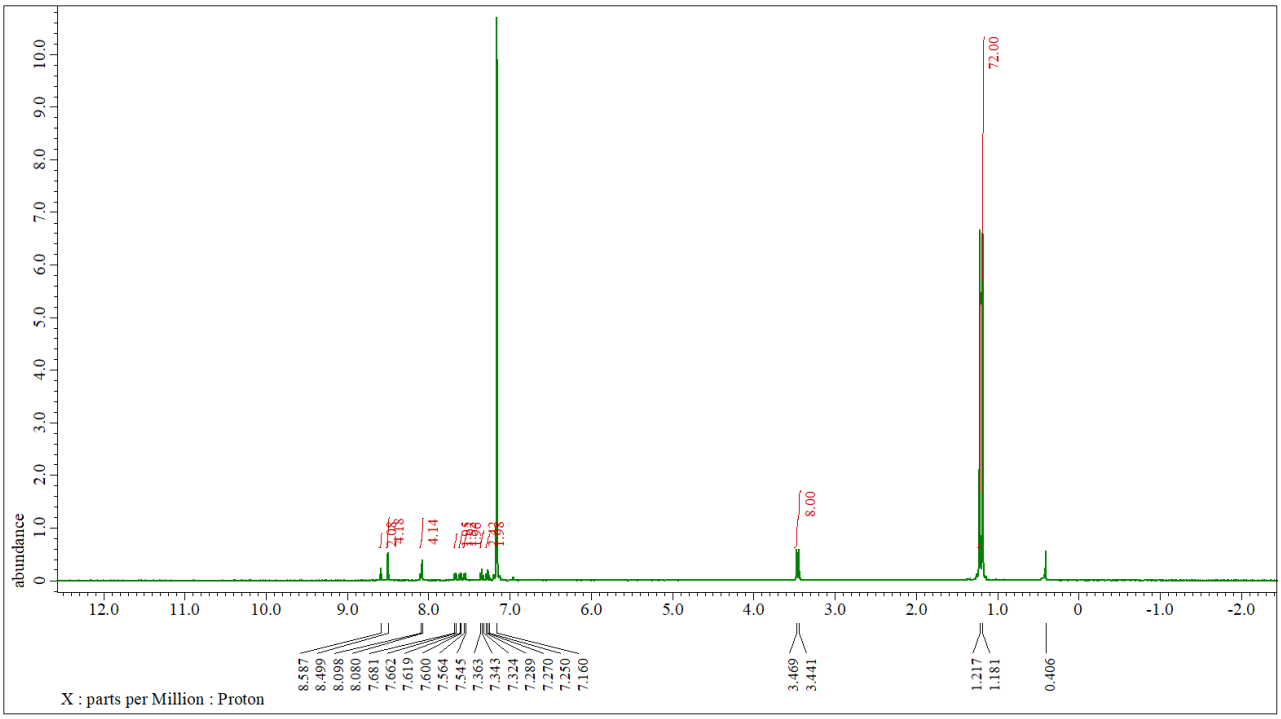

Figure S9. ^{1}H NMR spectrum of **4**.

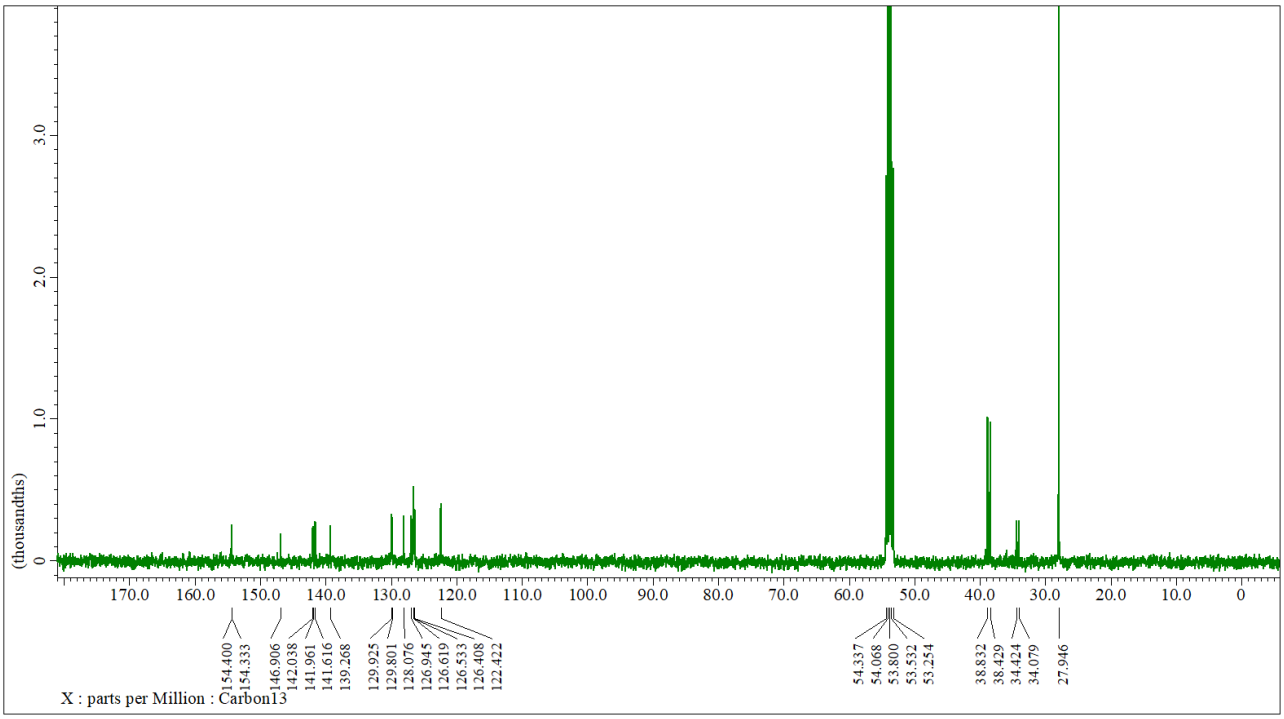

Figure S10. ^{13}C{^{1}H} NMR spectrum of **4**.

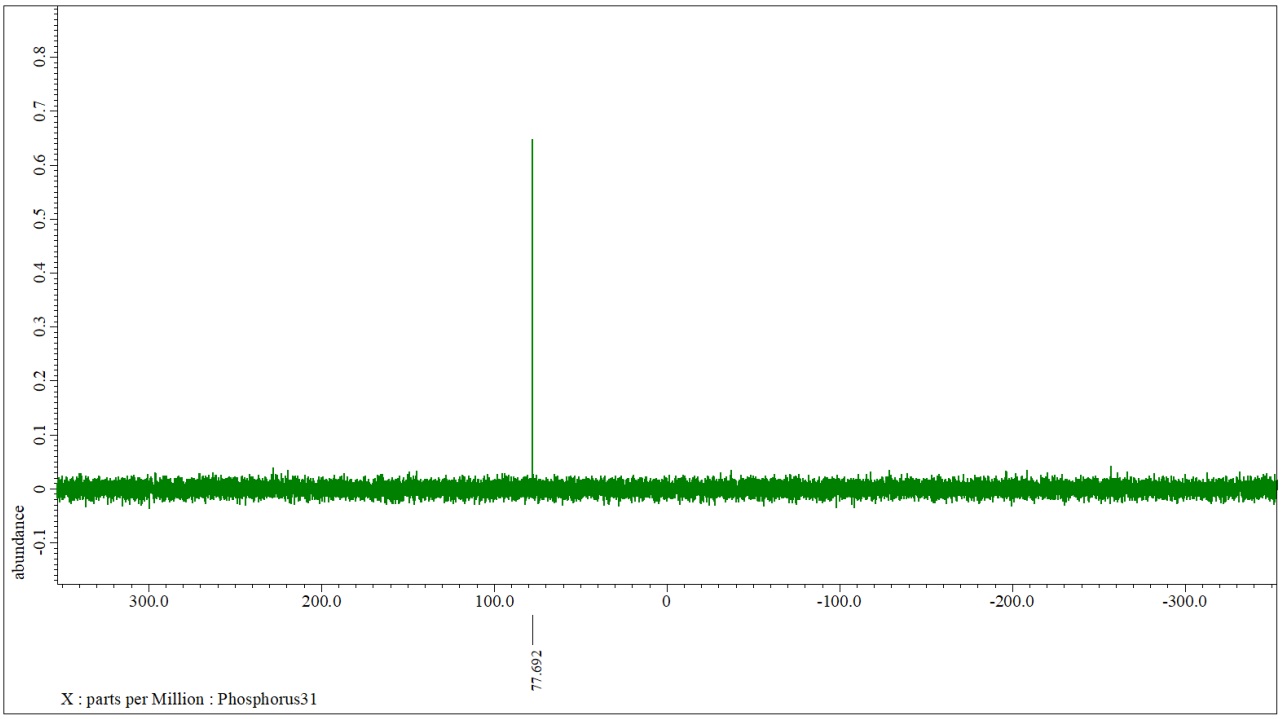

Figure S11. $^{31}P\{^{1}H\}$ NMR spectrum of **4**.

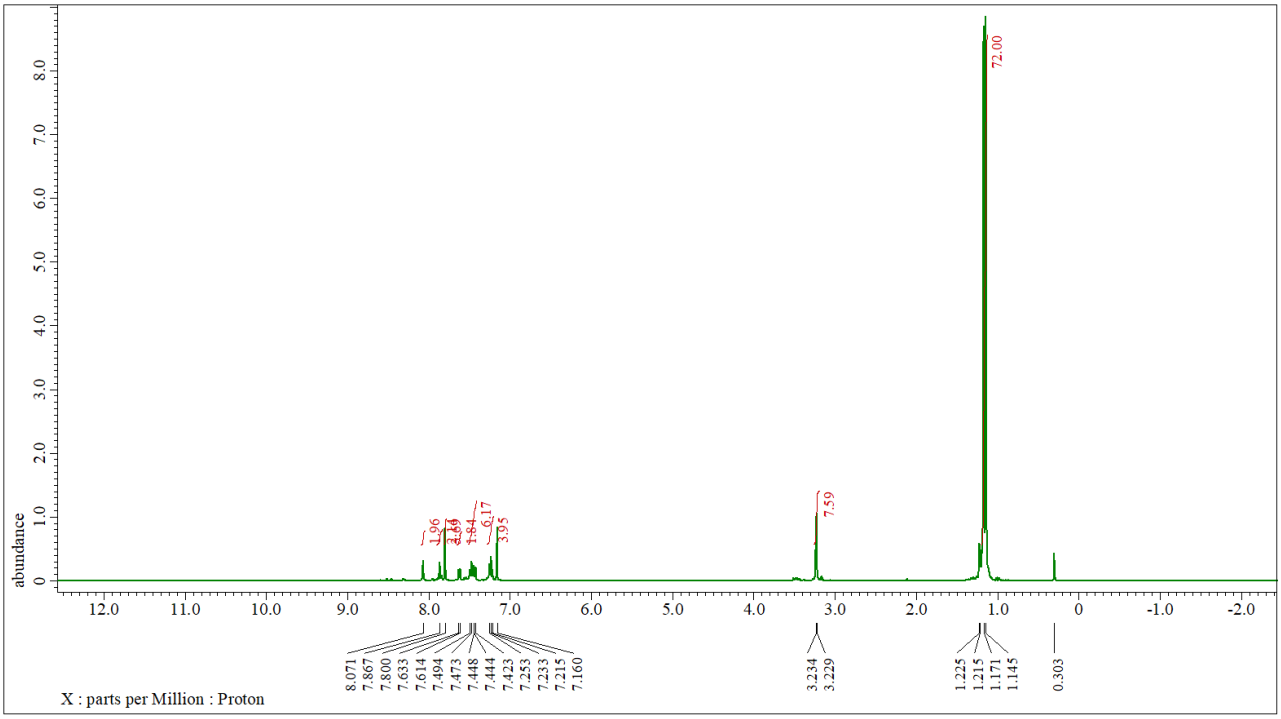

Figure S12. ^{1}H NMR spectrum of **5**.

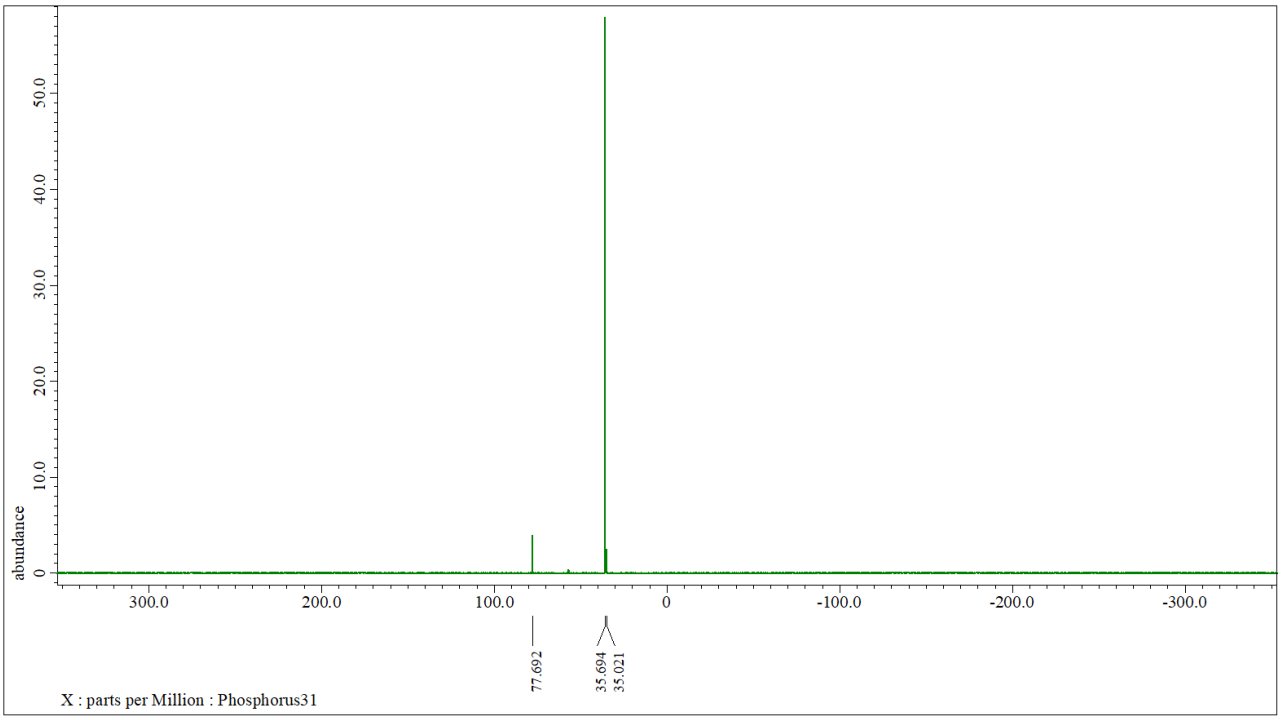

Figure S13. ^{31}P{^{1}H} NMR spectrum of **5**.

Computational Details.

Density-functional-theory (DFT) calculations were performed with the Gaussian 09 program (Rev. E01).[S13] All geometry optimizations were carried out with the B3LYP functional with the Grimme's dispersion correction (B3LYP-D3).[S14-18] We employed the SDD (Stuttgart/Dresden pseudopotentials) basis set[S19,20] for Mo and I and the 6-31G(d) basis set[S21-24] for the other atoms, respectively. All stationary-point structures were confirmed to have the appropriate number of imaginary frequencies by vibrational analysis. An appropriate connection between a reactant and a product was confirmed by quasi-IRC calculations. In the quasi-IRC calculation, the geometry of a transition state was shifted by perturbing the geometries very slightly along the reaction coordinates and released for equilibrium optimization. To discuss the energetics of the cleavage of an Mo–N_2 bond of **I**, **II**, and **C**, and the N≡N bond cleavage of **II** and **C**, single-point energy calculations were performed for all optimized structures using the SDD and the 6-311+G(d,p) basis sets. [S25-27] In the single-point calculations, solvation effects of THF (ε = 7.4257) were taken into account by using the polarizable continuum model (PCM).[S28] Detailed data on SCF energies, thermal energy corrections at 298 K, and SCF energies in THF are listed in Table S5.

For the cleavage of an Mo–N_2 bond of **I**, **II**, and **C** described in Figures S14-S16, we optimized the corresponding products, in which an MoI(PNP) unit was completely separated from the remaining MoI(N_2)(PNP) unit. Unfortunately, all our attempts to locate transition states of the Mo–N_2 bond dissociation have failed. This is because even when an MoI(PNP) unit was separated from the bridging N_2 ligand by 5 Å in an initial structure, an Mo–N≡N–Mo structure (reactant) was recovered during optimization. On the other hand, we successfully found transition states for the N≡N bond cleavage of **II** and **C** as presented in Figures S17 and S18.

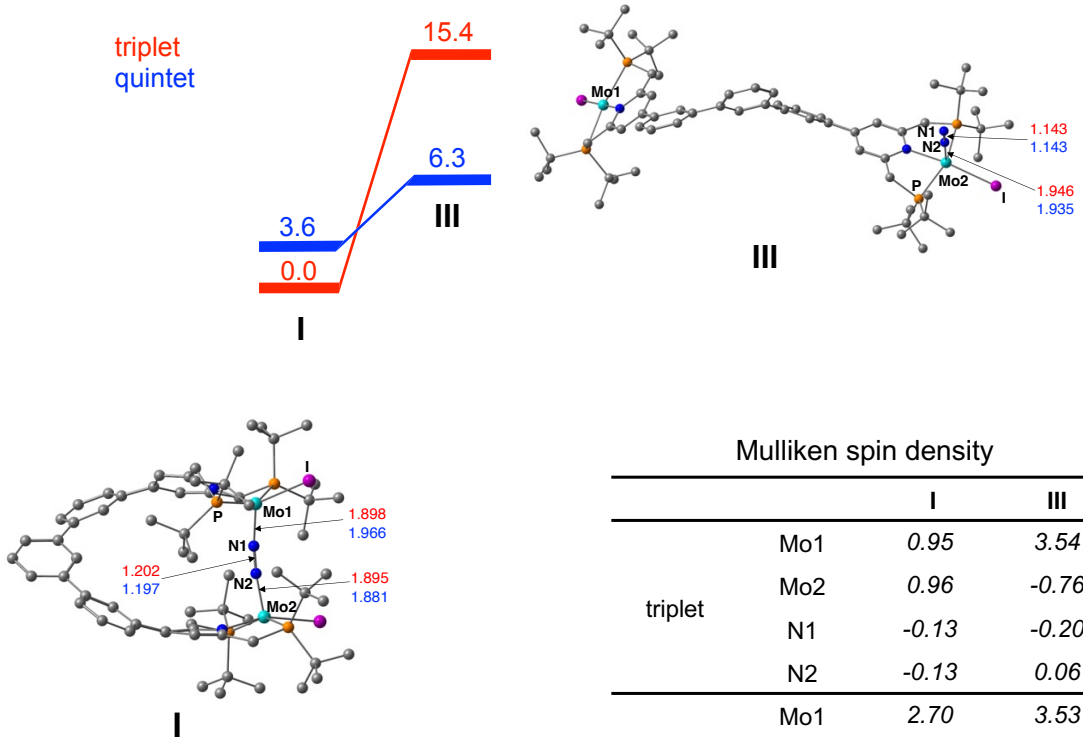

Mulliken spin density

		I	III
triplet	Mo1	*0.95*	*3.54*
	Mo2	*0.96*	*-0.76*
	N1	*-0.13*	*-0.20*
	N2	*-0.13*	*0.06*
quintet	Mo1	*2.70*	*3.53*
	Mo2	*0.98*	*1.05*
	N1	*-0.16*	*-0.01*
	N2	*-0.15*	*-0.03*

Figure S14. Free energy profile calculated at 298.15 K (ΔG_{298} kcal/mol in THF) for dissociation of an Mo-N_2 bond of **I** yielding **III**, together with optimized structures of **I** and **III**. Hydrogen atoms attached to carbon atoms are omitted for clarity. Selected bond distances are given in Å. Mulliken spin densities assigned to the Mo atoms and the bridging N_2 ligand are also presented in italics.

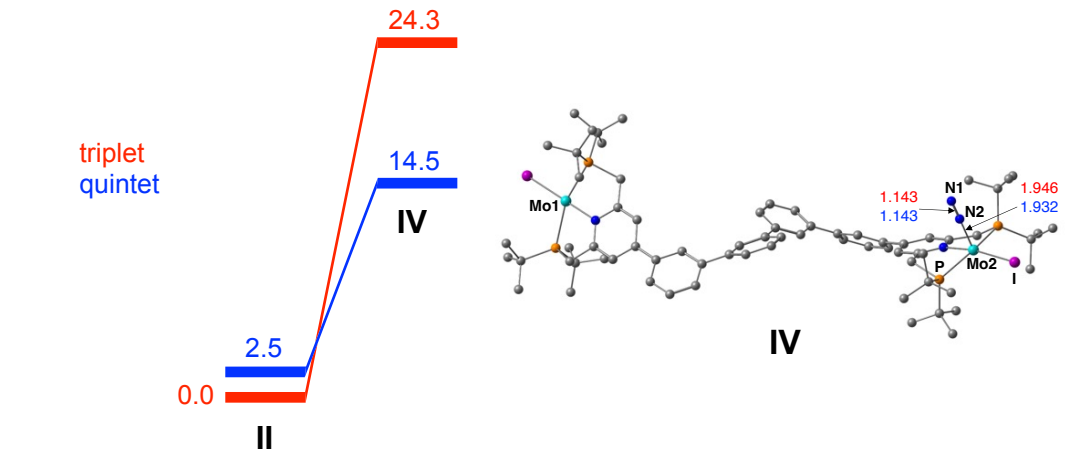

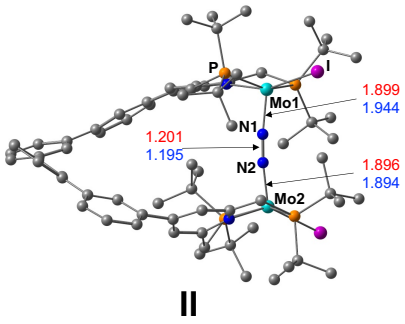

Mulliken spin density

		II	IV
triplet	Mo1	*0.96*	*3.52*
	Mo2	*0.98*	*-0.77*
	N1	*-0.12*	*-0.20*
	N2	*-0.14*	*0.06*
quintet	Mo1	*2.53*	*3.52*
	Mo2	*1.05*	*1.05*
	N1	*-0.15*	*-0.01*
	N2	*-0.16*	*-0.03*

Figure S15. Free energy profile calculated at 298.15 K (ΔG_{298} kcal/mol in THF) for dissociation of an Mo-N_2 bond of **II** yielding **IV**, together with optimized structures of **II** and **IV**. Hydrogen atoms attached to carbon atoms are omitted for clarity. Selected bond distances are given in Å. Mulliken spin densities assigned to the Mo atoms and the bridging N_2 ligand are also presented in italics.

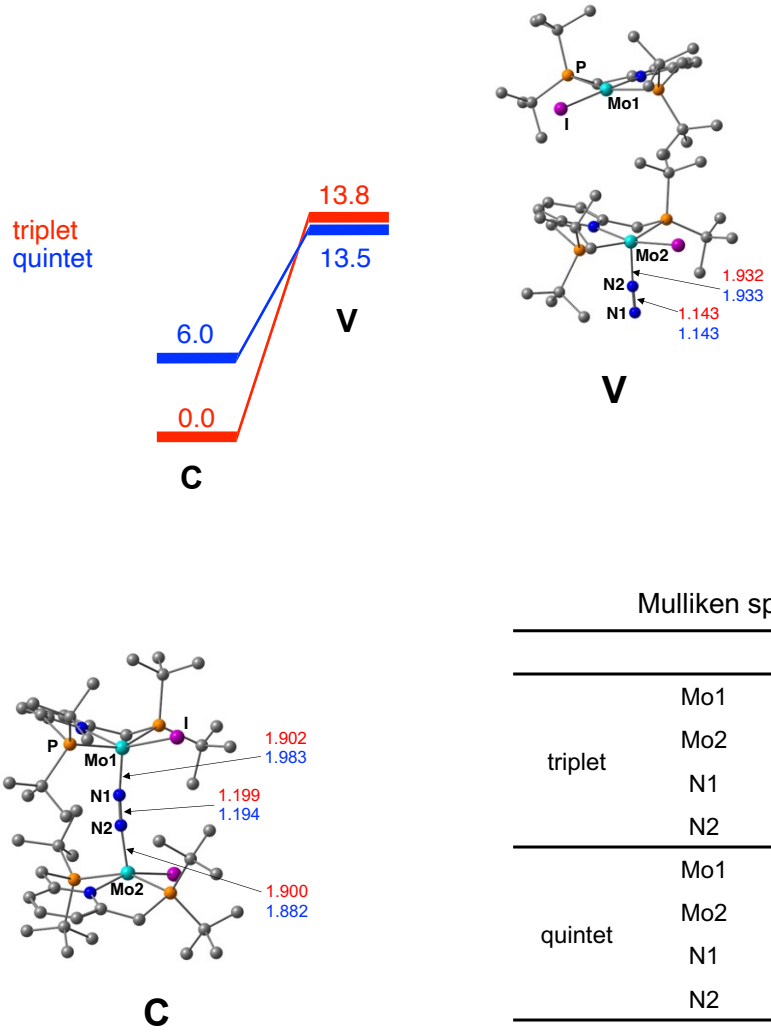

Mulliken spin density

		C	V
triplet	Mo1	*1.03*	*3.43*
	Mo2	*1.02*	*-1.05*
	N1	*-0.13*	*0.02*
	N2	*-0.14*	*0.03*
quintet	Mo1	*2.84*	*3.43*
	Mo2	*0.94*	*1.05*
	N1	*-0.16*	*-0.02*
	N2	*-0.14*	*-0.03*

Figure S16. Free energy profile calculated at 298.15 K (ΔG_{298} kcal/mol in THF) for dissociation of an Mo-N_2 bond of **C** yielding **V**, together with optimized structures of **C** and **V**. Hydrogen atoms attached to carbon atoms are omitted for clarity. Selected bond distances are given in Å. Mulliken spin densities assigned to the Mo atoms and the bridging N_2 ligand are also presented in italics.

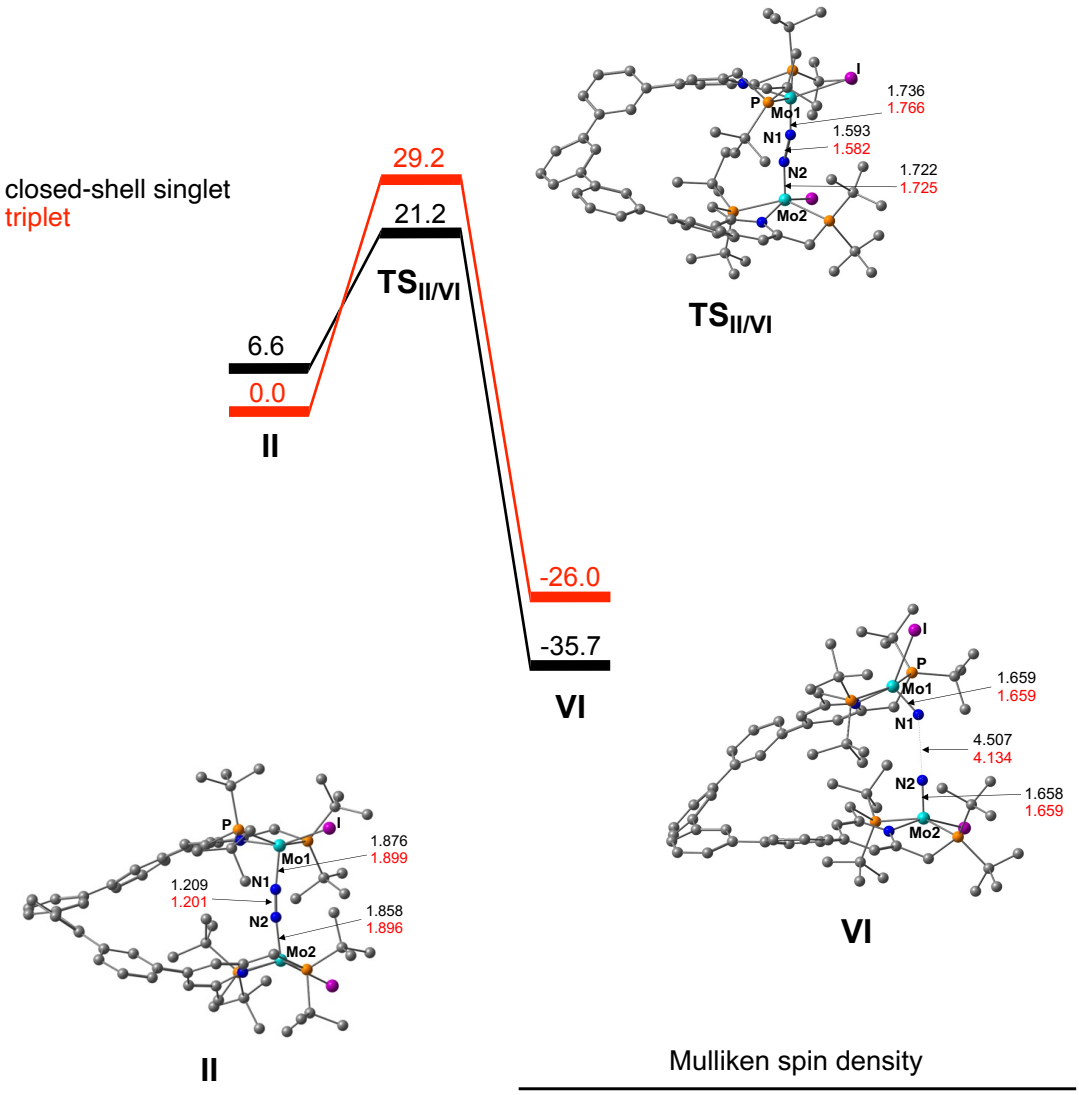

Mulliken spin density

		II	TS$_{II/VI}$	VI
triplet	Mo1	*0.96*	*1.37*	*1.12*
	Mo2	*0.98*	*-0.22*	*0.00*
	N1	*-0.12*	*-0.09*	*0.00*
	N2	*-0.14*	*0.03*	*-0.11*

Figure S17. Free energy profile calculated at 298.15 K (ΔG_{298} kcal/mol in THF) for the N≡N bond cleavage of the bridging dinitrogen ligand in **II** yielding **VI**, together with optimized structures of **II**, transition state (**TS$_{II/VI}$**) and **VI**. Hydrogen atoms attached to carbon atoms are omitted for clarity. Selected bond distances are given in Å. Mulliken spin densities assigned to the Mo atoms and the bridging N_2 ligand in the triplet state are presented in italics.

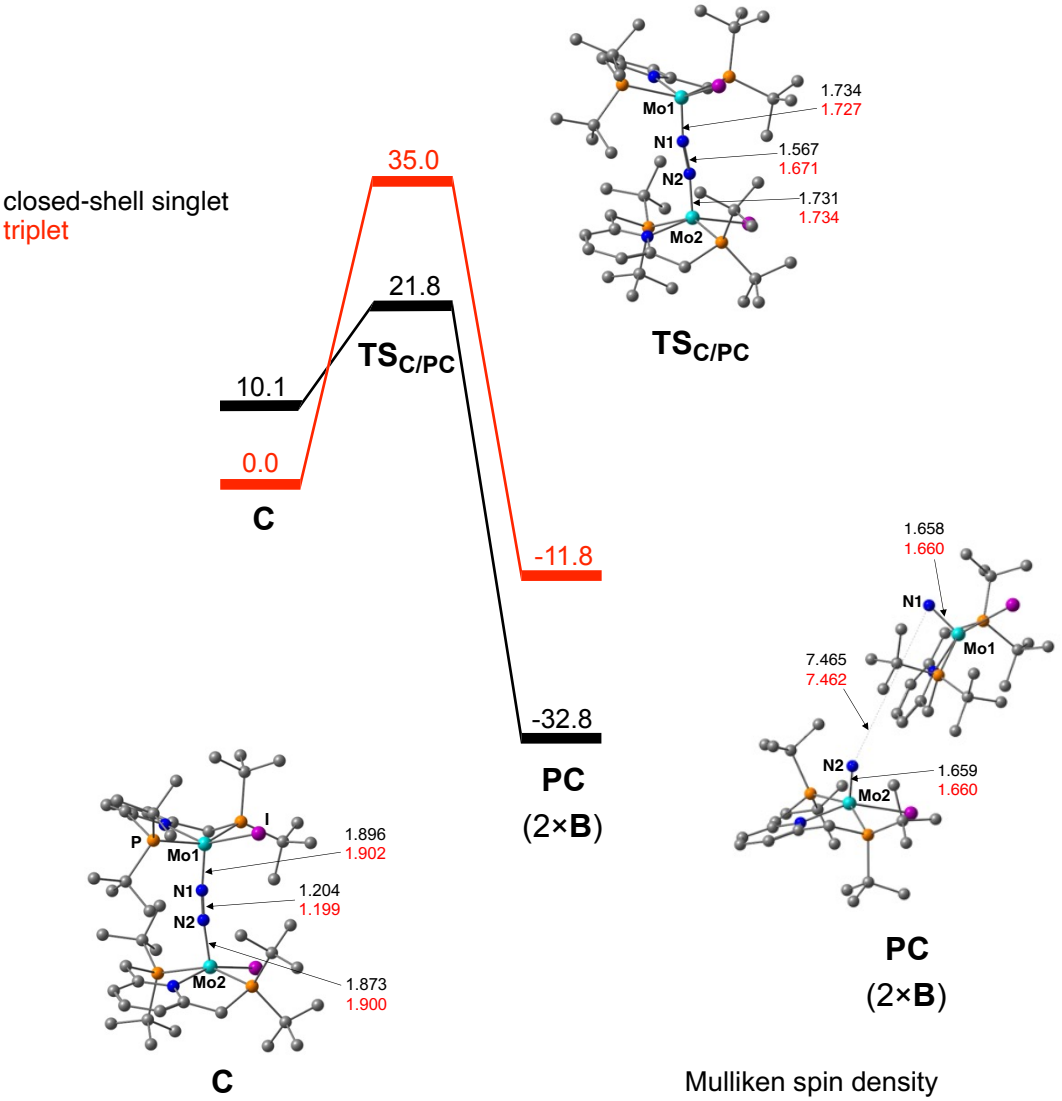

Mulliken spin density

		C	TS$_{C/PC}$	PC
triplet	Mo1	*1.03*	*0.26*	*0.00*
	Mo2	*1.02*	*1.00*	*1.17*
	N1	*-0.13*	*0.00*	*0.00*
	N2	*-0.14*	*-0.02*	*-0.09*

Figure S18. Free energy profile calculated at 298.15 K (ΔG_{298} kcal/mol in THF) for the N≡N bond cleavage of the bridging dinitrogen ligand in **C** yielding **PC** (or two molecules of **B**), together with optimized structures of **C**, transition state (**TS$_{C/PC}$**) and **PC**. Hydrogen atoms attached to carbon atoms are omitted for clarity. Selected bond distances are given in Å. Mulliken spin densities assigned to the Mo atoms and the bridging N_2 ligand in the triplet state are presented in italics.

Table S5. SCF energies (*in vacuo*), thermal energy corrections at 298 K, SCF energies (in THF).

Species and spin states		SCF energy/hartree	Thermal corrections/hartree	SCF energy (in THF)/hartree
I	closed-shell singlet	-4240.81103875	1.373832	-4241.70315208
	triplet	-4240.81945180	1.375284	-4241.71237005
	quintet	-4240.81170478	1.372194	-4241.70355617
II	closed-shell singlet	-4471.88459228	1.448172	-4472.83808723
	triplet	-4471.89486556	1.448036	-4472.84853592
	quintet	-4471.88668785	1.443793	-4472.84025644
III	triplet	-4240.75738213	1.356105	-4241.66857249
	quintet	-4240.77203208	1.356569	-4241.68356950
IV	triplet	-4471.82044248	1.430717	-4472.79245459
	quintet	-4471.83530827	1.430792	-4472.80826430
V	triplet	-3548.79273544	1.152659	-3549.52025683
	quintet	-3548.79280291	1.152259	-3549.52034643
$TS_{II/VI}$	closed-shell singlet	-4471.85870329	1.445290	-4472.81195121
	triplet	-4471.84420466	1.443222	-4472.79724227
VI	closed-shell singlet	-4471.93825086	1.446708	-4472.90411401
	triplet	-4471.91874080	1.438854	-4472.88079678
C	closed-shell singlet	-3548.81987802	1.162819	-3549.53633315
	triplet	-3548.83343583	1.163178	-3549.55277254
	quintet	-3548.82241780	1.159785	-3549.53975149
$TS_{C/PC}$	closed-shell singlet	-3548.79820293	1.160572	-3549.51547145
	triplet	-3548.77320571	1.156874	-3549.49073155

PC (2×B)	closed-shell singlet	-3548.86565467	1.157344	-3549.59924751
	triplet	-3548.83044817	1.153373	-3549.56179639

6. Supplementary references.

S1. G. A. Bain and J. F. Berry, *J. Chem. Educ*., 2008, **85**, 532-536.

S2. S. Kuriyama, K. Arashiba, K. Nakajima, H. Tanaka, N. Kamaru, K. Yoshizawa and Y. Nishibayashi, *J. Am. Chem. Soc.* 2014, **136**, 9719-9731.

S3. F. Stoffelbach, D. Saurenz and R. Poli, *Eur. J. Inorg. Chem.,* 2001, 2699-2703.

S4. R. Poli, S. T. Krueger, S. P. Mattamana, K. R. Dunbar and Z. Hanhua, *Inorg. Synth.,* 1998, **32**, 198-203.

S5. K. Arashiba, Y. Miyake and Y. Nishibayashi, *Nat. Chem.,* 2011, **3**, 120–125.

S6. P. L. Watson, T. H. Tulip and I. Williams, *Organometallics,* 1990, **9**, 1999-2009.

S7. M. W. Weatherburn, *Anal. Chem.,* 1967, **39**, 971-974.

S8. CrystalStructure 4.3.1: Single Crystal Structure Analysis Software; Rigaku Corp: Tokyo, Japan, and MSC: The Woodlands, TX, 2018.

S9. M. C. Burla, R. Caliandro, M. Camalli, B. Carrozzini, G. L. Cascarano, C. Giacovazzo, M. Mallamo, A. Mazzone, G. Polidori and R. Spagna, *J. Appl. Cryst*., 2012, **45**, 357-361.

S10. G. M. Sheldrick, *Acta Crystallogr.,* 2008*,* **A64**, 112-122.

S11. G. M. Sheldrick, *Acta Crystallogr*., 2015, **C71**, 3-8.

S12. A. L. Spek, *Acta Crystallogr.,* 2015, **C71**, 9-18.

S13. *Gaussian 09, Revision E.01*: M. J. Frisch, G. W. Trucks, H. B. Schlegel, G. E. Scuseria, M. A. Robb, J. R. Cheeseman, G. Scalmani, V. Barone, B. Mennucci, G. A. Petersson, H. Nakatsuji, M. Caricato, X. Li, H. P. Hratchian, A. F. Izmaylov, J. Bloino, G. Zheng, J. L. Sonnenberg, M. Hada, M. Ehara, K. Toyota, R. Fukuda, J. Hasegawa, M. Ishida, T. Nakajima, Y. Honda, O. Kitao, H. Nakai, T. Vreven, J. A. Montgomery, Jr., J. E. Peralta, F. Ogliaro, M. Bearpark, J. J. Heyd, E. Brothers, K. N. Kudin, V. N. Staroverov, T. Keith, R. Kobayashi, J. Normand, K. Raghavachari, A. Rendell, J. C. Burant, S. S. Iyengar, J. Tomasi, M. Cossi, N. Rega, J. M. Millam, M. Klene, J. E. Knox, J. B. Cross, V. Bakken, C. Adamo, J. Jaramillo, R. Gomperts, R. E. Stratmann, O. Yazyev, A. J. Austin, R. Cammi, C. Pomelli, J. W. Ochterski, R. L. Martin, K. Morokuma, V. G. Zakrzewski, G. A. Voth, P. Salvador, J. J. Dannenberg, S. Dapprich, A. D. Daniels, O. Farkas, J. B. Foresman, J. V. Ortiz, J. Cioslowski, and D. J. Fox, Gaussian, Inc.: Wallingford CT, 2013.

S14. Becke, A. D. *Phys. Rev. A,* 1988, **38**, 3098-3100.

S15. Becke, A. D. *J. Chem. Phys.,* 1993, **98**, 5648-5642.

S16. Lee, C.; Yang, W.; Parr, R. G. *Phys. Rev. B,* 1988, **37**, 785-789.

S17. Vosko, S. H.; Wilk, L.; Nusair, M. J. *Can. J. Phys.,* 1980, **58**, 1200-1211.

S18. Grimme, S.; Antony, J.; Ehrlich, S.; Krieg, H. *J. Phys. Chem.,* 2010, **132**, 154104.

S19. Dolg, M.; Wedig, U.; Stoll, H.; Preuß, H. *J. Chem. Phys*., 1987, **86**, 866-872.

S20. Andrae, D.; Häußermann, U.; Dolg, M.; Stoll, H.; Preuß, H. *Theor. Chim. Acta.,* 1990, **77**, 123-141.

S21. Ditchfield, R.; Hehre, W. J.; Pople, J. A. *J. Chem. Phys*., 1971, **54**, 724-728.

S22. Hehre, W. J.; Ditchfield, R.; Pople, J. A. *J. Chem. Phys.,* 1972, **56**, 2257-2261.

S23. Hariharan, P. C.; Pople, J. A. *Theor. Chem. Acc.,* 1973, **28**, 213-222.

S24. Francl, M. M.; Pietro, W. J.; Hehre, W. J.; Binkley, J. S.; Gordon, M. S.; DeFrees, D. J.; Pople, J. A. *J. Chem. Phys*., 1982, **77**, 3654-3665.

S25. Krishnan, R.; Binkley, J. S.; Seeger, R.; Pople, J. A., *J. Chem. Phys*., 1980, **72**, 650-654.

S26. McLean, A. D.; Chandler, G. S., *J. Chem. Phys*., 1980, **72**, 5639-5648.

S27. Clark, T.; Chandrasekhar, J.; Spitznagel, G. W.; Schleyer, P. v. R., *J. Comput. Chem*., 1983, **4**, 294-301.

S28. Tomasi, J.; Mennucci, B.; Cammi, R. *Chem. Rev*., 2005, **105**, 2999-3094.